is a reasonable result. As the number of desorption sites decreases, the observed value of τ_0 would increase.

Contamination Effects. A decrease in τ values with contaminated surfaces has been observed in these studies with desorption of CsCl and CsI as well as in the case of desorption of U^{24} and U^+.[25] Studies by Scheer and Fine[5] of desorption of Cs^+ resulting from Cs, CsCl, and CsI adsorbed on W and Re surfaces showed that τ increased when the surface was contaminated. An explanation of the decrease observed in the present studies with contamination of the surface is given by considering that more desorption sites are present with more impurities on the surface. Fewer random walk steps would be required in step 3. In the studies of Scheer and Fine, large values of ΔH^* were observed which would lead one to believe that step 1 is probably the rate-determining step in their desorption process. The addition of contaminates to the surface in the studies of Scheer and Fine would not be expected to have the same effect since the rate-determining step is step 1 rather than step 3.

Acknowledgments. The authors gratefully acknowledge financial support for this research from the National Science Foundation through Grants No. GH-35938 and GH-42513.

Thanks are given also to Dr. Leo W. Huang for his work on preparation of the Ni(100) surfaces and some scanning electron microscopy performed at the University of Wisconsin—Milwaukee. Professor William Warke of the Illinois Institute of Technology is thanked for his help with scanning electron microscopy of the surfaces used in this study.

References and Notes

(1) Based on a thesis by M. B. Liu submitted in partial fulfillment of the requirements for the Ph.D. Degree, Illinois Institute of Technology, Chicago, Ill., 1974.
(2) L. W. Huang and P. G. Wahlbeck, *J. Phys. Chem.*, preceding paper in this issue.
(3) (a) G. E. Cogin and G. E. Kimball, *J. Chem. Phys.*, **11**, 1035 (1948). (b) M. D. Scheer and J. Fine, *ibid.*, **36**, 1647 (1962).
(4) G. M. Rothberg, M. Eisenstadt, and P. Kusch, *J. Chem. Phys.*, **30**, 517 (1959).
(5) M. D. Scheer and J. Fine, *J. Chem. Phys.*, **38**, 307 (1963).
(6) D. R. Stull and H. Prophet, *Natl. Stand. Ref. Data Ser., Natl. Bur. Stand.*, **No. 37**, 2nd ed (1971).
(7) S. A. Rice and W. Klemperer, *J. Chem. Phys.*, **27**, 573 (1957).
(8) R. F. Barrow and A. D. Caunt, *Proc. R. Soc. London, Ser. A*, **219**, 120 (1953).
(9) H. Honig, M. Mandel, M. L. Stitch, and C. H. Townes, *Phys. Rev.*, **96**, 629 (1954).
(10) A. G. Gaydon, "Dissociation Energies and Spectra of Diatomic Molecules", 3d ed, Chapman and Hall, London, 1968.
(11) J. G. Allpress and J. V. Sanders, *Surface Sci.*, **7**, 1 (1967).
(12) J. R. Anderson and R. J. MacDonald, *J. Catal.*, **13**, 345 (1969).
(13) L. H. Germer, E. J. Scheibner, and C. P. Hartman, *Phil. Mag.*, **5**, 222 (1960).
(14) L. H. Germer and A. V. MacRae, *J. Appl. Phys.*, **33**, 2923 (1962).
(15) L. H. Germer and A. V. MacRae, *J. Chem. Phys.*, **36**, 1555 (1962).
(16) D. A. Degras, *Suppl. Nuovo Cim.*, **5**, 408 (1967).
(17) A. M. Horgen and D. A. King in "The Structure and Chemistry of Solid Surfaces", G. A. Somorjai, Ed., Wiley, New York, N.Y., 1969.
(18) G. Blyholder, *J. Chem. Phys.*, **62**, 3193 (1975).
(19) G. Blyholder, *J. Phys. Chem.*, **79**, 756 (1975).
(20) G. Ehrlich and F. G. Hudda, *J. Chem. Phys.*, **35**, 1421 (1961).
(21) O. Knacke and I. N. Stranski, *Prog. Metal Phys.*, **6**, 181 (1956).
(22) C. A. Hultman and G. M. Rosenblatt, *Science*, **188**, 145 (1975).
(23) E. A. Moelwyn-Hughes, "Physical Chemistry", 2d ed, Pergamon Press, New York, N.Y., 1961, p 959.

An Electron Spin Resonance Study of the Pressure Dependence of Ordering and Spin Relaxation in a Liquid Crystalline Solvent[1]

James S. Hwang, K. V. S. Rao, and Jack H. Freed*

Department of Chemistry, Cornell University, Ithaca, New York 14853 *(Received December 17, 1975)*

An ESR study of ordering and relaxation as a function of pressure is reported for the perdeuterated Tempone nitroxide radical probe in phase V solvent. The study of ordering focuses on the nature of the intermolecular interactions between the probe and solvent (and between solvent molecules), which lead to the weak ordering of the probe. The results are suggestive of longer range interactions than were previously found by McColl in an NMR study on a pure solvent. The spin relaxation results have been analyzed in terms of activated-state theory to obtain values of ΔH_a and ΔV_a as a function of T and P for the rotational reorientation. Anomalous features of the spin relaxation previously reported by Polnaszek and Freed in a temperature-dependent study of this system are reported here as a function of pressure. These anomalies are most pronounced for rotational correlation times (τ_R) large enough that ESR line shapes are no longer motionally averaged (i.e., they are characteristic of the slow motional region). In general, the anomalous behavior depends mainly on τ_R and appears to be nearly independent of the particular combination of T and P. A mechanism in which the local structure around the probe relaxes more slowly than the probe, as proposed by Polnaszek and Freed, is taken to be the most likely explanation. Rapid motional effects in the rigid solvent are also reported. Details of the high-pressure accessory are given.

1. Introduction

ESR relaxation studies can supply useful information about molecular dynamics in condensed media. We have actively conducted careful studies of such processes in both isotropic and anisotropic (liquid crystalline) environments,[2-6] over a wide range of temperatures, embracing the fast motional region to the rigid limit. Some NMR studies have demonstrated the utility of experiments over a wide range of pressures to learn about molecular dynamics.[7,8] However, there are few comparable ESR studies.[9] In this work, we complement our previous experiments on temperature dependence, in which

line shapes consistent with non-Brownian reorientational motion (e.g., large angle jump diffusion) and anomalous frequency dependences of the rotational reorientational correlation functions were observed, with a study of pressure dependence. This complementary study has yielded results which aid in interpreting the previous observations. For example, we can ask such questions as to whether "pressure-induced" slow-motional spectra will be consistent with the same or different non-Brownian motional models; or whether anomalous frequency-dependent line width behavior also exists as a function of pressure.

The primary effect of increasing pressure at constant temperature is to increase the intermolecular potentials, while measurements at constant pressure, in which temperature is varied, include combined effects of molecular kinetic energies and intermolecular potentials. Thus, the pressure-dependent experiments are more directly amenable to analysis in terms of molecular models. [Of course representations of the experiments at constant volume are of considerable utility, but this requires the knowledge of PVT data.] Furthermore, as reviewed by Jonas,[7] pressure-dependent experiments are very useful in distinguishing between spin relaxation effects due to internal motions from those due to overall motions. This is of particular importance in assigning anomalous relaxation behavior.

We have, in this work, studied the spin-probe PD-Tempone in the liquid crystalline solvent phase V. We have shown in previous extensive studies at atmospheric pressure with a variety of isotropic and nematic liquid solvents that, by the use of this perdeuterated spin probe, one removes most of the undersirable width inhomogeneity typical of spin probes. This yields better resolved spectra, which can be analyzed with much greater confidence and accuracy. Also, it was found in our previous studies with this probe that the magnetic tensors are very nearly identical in a variety of nonhydrogen-bonding solvents, including nematic solvents,[3-5] and we take this to imply that there are little or no specific interactions with the nitroxide entity in such solvents that might confuse our interpretations. We chose phase V solvent for this initial study as a function of pressure, because it was the only nematic solvent that in our previous studies[5] had the properties of (1) having a nematic phase over a wide temperature range and (2) being viscous enough at its lower temperatures that spectra characteristic of the slow motional region were observed. These properties were expected to be manifested as a function of pressure.

It is possible, with nematic solvents, to study thermodynamic properties related to the measured order parameter as a function of T and P (or T and V), and one may interpret them in terms of statistical theories of the nematic state. There have been a few such NMR studies of nematics,[10-12] although this work is the first such ESR study. Thus, while our experiments were conceived primarily for studies of molecular dynamics, we also discuss our results on ordering to indicate their relevance to nematic equations of state.

The experimental aspects, including a description of the high-pressure system, are given in section 2. Our results on ordering vs. T and P are given in section 3, where they are discussed in terms of simple mean field theory. The spin relaxation results are presented and discussed in section 4. Conclusions appear in section 5.

2. Experimental Methods

Spectra of PD-Tempone in phase V at X-band were obtained with a Varian E-12 spectrometer modified for high pressures and interfaced with a PDP-9 computer. The details of interfacing are discussed in ref 3. The high-pressure experiments were carried out in a thermostated Be–Cu vessel containing a slow-wave helix, and a pair of modulation coils mounted on a Teflon modulation capsule. The high-pressure system was designed for 10 kbars maximum pressure, but the actual maximum pressures required in this work (e.g., 4.5 kbars for phase V at 45 °C) were determined by the freezing point of the nematic phase of phase V.

The high-pressure generating system is capable of delivering 14 l. of high-pressure fluid continuously without being disconnected from the vessel. The schematic of the high-pressure generating system is given in Figure 1. Pressures up to 4 kbars can be conveniently generated with a Haskel DSXHW-602 air driven liquid pump. This is performed with valves 1 and 2 closed and valve 3 open. For pressures in excess of 4 kbars (and up to 10 kbars), a Harwood A2.5J high-pressure intensifier is brought into the circuit by closing valve 3 and opening valve 2.

We show in Figure 2 the assembled ESR high-pressure vessel which was tested up to 7 kbars. The vessel is machined from a 2-in. rod of temper H Berylco 25. The rod was tested ultrasonically before machining using an immersion method. After machining, the finished parts were heat treated (at 600 °F for 2 h) using a precipitation hardening process. Earlier work on the use of Berylco 25 for a high-pressure ESR vessel has been discussed by Plachy and Schaafsma[13] and by Doyle et al.[14] for a high-pressure ENDOR cavity. The microwave and pressure plugs, which seal the ESR vessel at both ends, employ true Bridgman seals,[15] which cause minimal wear on the seals and yield a vessel virtually free of leaks.[16] The microwave plug was designed for variable frequency experiments from S-band to X-band.

Variable temperature and high pressure experiments were performed using a brass temperature control jacket constructed to fit around the pressure vessel. This system was made leak tight by means of a rubber sealant. The temperature of the solution in the variable temperature jacket was monitored with a copper–constantan thermocouple or (when accurate temperature reading to 0.1 °C is required) a precision thermistor. The solution, which flows into the copper tubings of the temperature control jacket, is from a Tamson constant temperature bath, with temperature stability to within 0.01 °C. The temperature in the temperature control jacket is constant to within 0.1 °C and has a temperature range from −25 to 75 °C.

The sample preparation and sample holder containing a helix are similar to the description given elsewhere.[9] The solutions of PD-Tempone in phase V were somewhat more concentrated than previously used in I in order to enhance sensitivity. Some spin exchange, therefore, was present at the higher temperatures near atmospheric pressure, but it was still possible to introduce the appropriate line shape corrections for inhomogeneous deuteron broadening[3,5] in the presence of spin exchange in the manner of Lang and Freed.[17]

Most of the other aspects of the experimental methods are as discussed in I; e.g., the magnetic tensor components used for PD-Tempone in phase V are those given in I.

3. Order Parameters and Statistical Thermodynamic Relations

The nominal ordering parameters $\langle \boldsymbol{D}^2_{00} \rangle_z \equiv S^{(p)}$ determined for PD-Tempone in phase V, appropriate for a one parameter potential,[5] are plotted vs. pressure in Figure 3. [The $\boldsymbol{D}^L_{KM}(\Omega)$ are the generalized spherical harmonics, cf. ref 2–5, and the

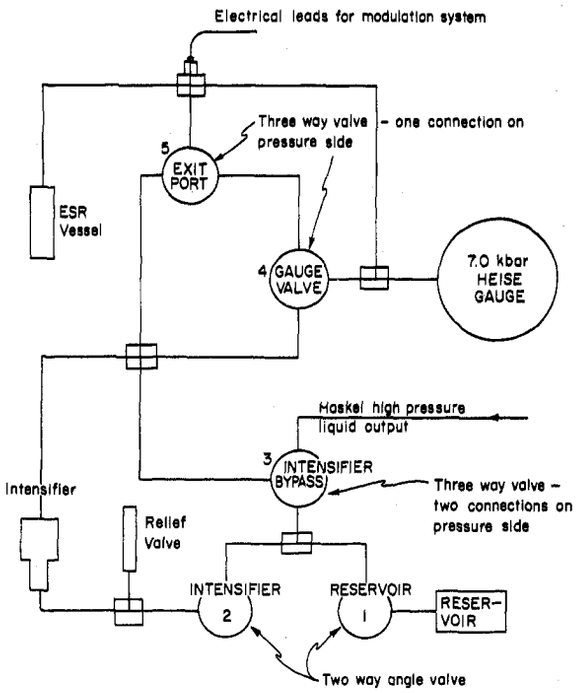

Figure 1. Schematic of the high pressure generating system.

angular brackets imply ensemble averaging.] These results are from the measured hyperfine shifts and are computed from eq 2.27a of I (with β' the tilt angle of the magnetic z axis with respect to the ordering z' axis set equal to zero). It is seen to vary linearly with pressure. (The significant deviations from linearity at high pressures are due to the fact that the data have not been corrected for the effects of slow tumbling and are not otherwise anomalous, cf. I.) In an NMR study on PAA of $S^{(s)}$ (the order parameter of the pure solvent) with pressure at more elevated temperatures, the graphs were generally nonlinear.[11]

It was shown in I, that the ordering of the spin probe is usually not axially symmetric, so that a pair of order parameters $\langle \boldsymbol{D}^2_{0,0} \rangle_z$ and $\langle \boldsymbol{D}^2_{2,0} + \boldsymbol{D}^2_{-2,0} \rangle_z$ (and the principal axes) must be specified. These may be determined from combined hyperfine and g shift measurements and eq 2.26 of I. However, it was not conveniently possible to measure very accurate g values in the high-pressure vessel. It was therefore assumed for convenience that the nominal $\langle \boldsymbol{D}^2_{0,0} \rangle_z$ value shown in Figure 3 may be replaced by the associated pair of order parameters found in I for the same nominal $\langle \boldsymbol{D}^2_{0,0} \rangle$ in the same system at atmospheric pressure (or more precisely the vapor pressure of solvent) and different temperatures. This would follow if, while the extent of ordering is affected by T and P, the "symmetry" of the molecular alignment remains about the same for a given extent of ordering. The basis of the two-term ordering tensor is[5]

$$\langle \boldsymbol{D}^L_{KM}(\Omega) \rangle = \int d\Omega P_0(\Omega) \boldsymbol{D}^L_{KM}(\Omega) \tag{3.1}$$

where $P_0(\Omega)$, the equilibrium distribution in Euler angles Ω between the molecular coordinate system and the laboratory system, is given by

$$P_0(\Omega) = \exp(-U(\Omega)/kT) / \int d\Omega \exp(-U(\Omega)/kT) \tag{3.2}$$

with $U(\Omega)$ the mean restoring potential of the probe in the field of nematic solvent molecules, which is given by

$$U(\alpha, \beta, 0)/kT \simeq -\lambda \cos^2 \beta - \rho \sin^2 \beta \cos 2\alpha \tag{3.3}$$

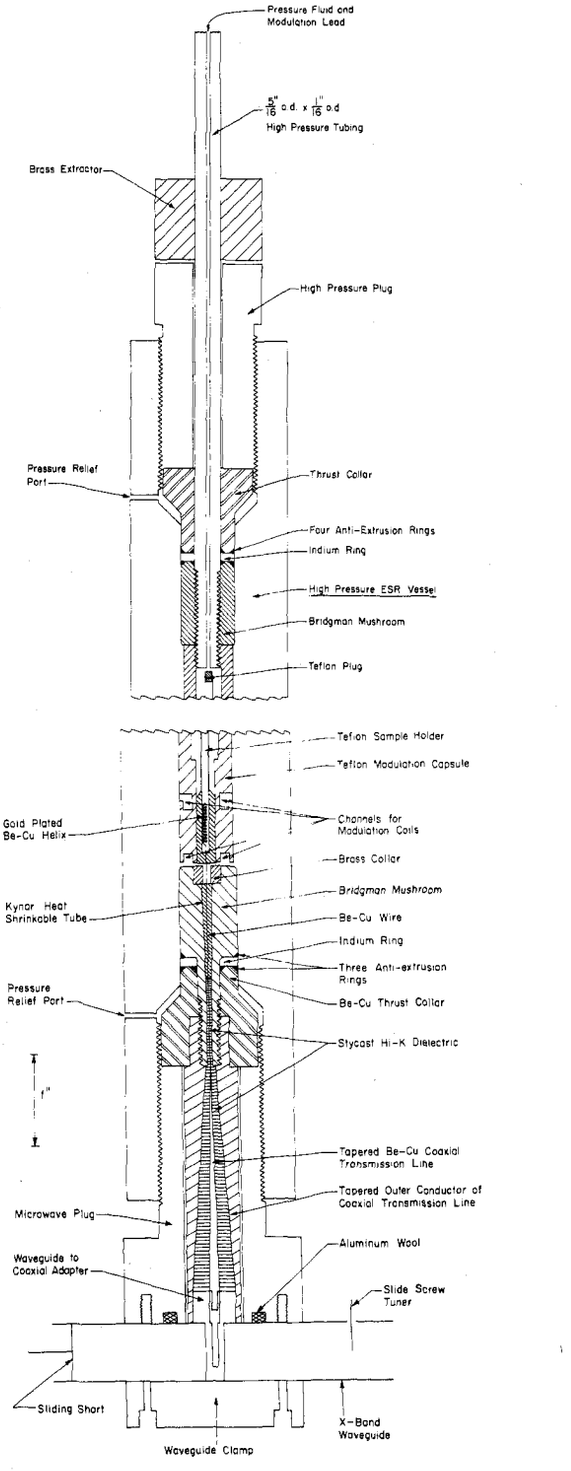

Figure 2. ESR high pressure vessel fully assembled. (The upper and lower halves are shown separately but are actually joined at the break lines.)

The Maier–Saupe-type form of the potential comes about when $\rho = 0$ in eq 3.3. Note that the mean torque on the probe is derived by taking the appropriate gradient of $U(\Omega)$, i.e.

$$\mathbf{T} = +i\mathbf{M}U(\Omega) \tag{3.4}$$

where $\mathbf{M}$ is an angular gradient operator defined in I. Thus $U(\Omega)$ is statistically the potential of mean torque[18] (within an arbitrary energy zero) for the spin probe.

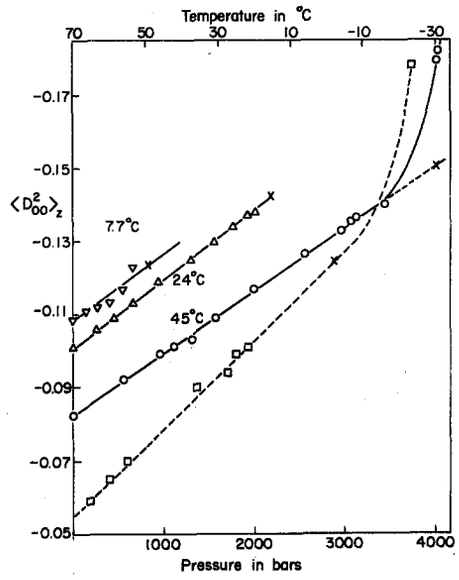

Figure 3. Nominal ordering parameter $\langle \boldsymbol{D}^{(2)}_{00} \rangle_z$ vs. pressure for PD-Tempone in phase V. The solid lines show least-squares fits. The dashed curve is for the temperature variation at 1 atm from Polnaszek and Freed. The nonlinear effects for larger ordering are due to onset of slow motion. The X's mark the melting points from the least-squares fits given in the text.

The values of $-\lambda_z$ and ρ_z obtained in this manner are shown in Figure 4. [The subscript z means that the molecular magnetic z axis is taken as the primary orientation axis.] They are linear in P, just as $S^{(p)}$ was. It was noted in I that the probe orients weakly with the magnetic z axis tending to be perpendicular to the director, the y axis tending to be parallel to the director, and the x axis tending to be oriented nearly at the magic angle.

Our results on ordering of the spin probe ($S^{(p)}$) as a function of T and P has some relevance for theories of the nematic state. First we note that, while the PD-Tempone spin probe is ordered to a lesser extent than the nematic solvent molecules themselves, it is indeed a probe of the surroundings. One often employs a "mean field" theory to estimate the true potential of mean torque U which is measured experimentally. Then one may make use of orientation-dependent expansions such as[19-23]

$$U^{(s)}_{mf}(\Omega) \simeq \sum_{\text{even L;K}} \bar{u}^{(ss)}_{L,K}(r) \langle \boldsymbol{D}^{L(s)}_{K,0}(\Omega') \rangle \boldsymbol{D}^{L(s)}_{K,0}(\Omega) \qquad (3.5)$$

and

$$U^{(p)}_{mf}(\Omega) \simeq \sum_{\text{even L,L';K,K'}} \bar{u}^{(sp)}_{L,L',K,K'}(r) \langle \boldsymbol{D}^{L(s)}_{K,0}(\Omega') \rangle \boldsymbol{D}^{L'(p)}_{K',0}(\Omega) \qquad (3.6)$$

where the subscripts mf imply mean field approximation, the superscripts (s) and (p) refer to solvent and probe, and we are assuming low concentrations of probe molecules, so the latter only interact with solvent molecules. The solvent order parameters $\langle \boldsymbol{D}^{L(s)}_{K,0}(\Omega') \rangle$ are determined by self-consistency considerations. The coefficients $\bar{u}^{(ij)}_{L,K}(r)$ are a measure of the strengths of the anisotropic interaction between molecules of species i and j and they are averages over the pair distribution function $n^{(2)}(r)$, e.g.

$$\bar{u}^{(ss)}_{L,K} = \rho^2 \int u^{(ss)}_{L,K}(r) n^{(2)}(r)\, dr \qquad (3.7)$$

where ρ is the number density. The other assumptions of such

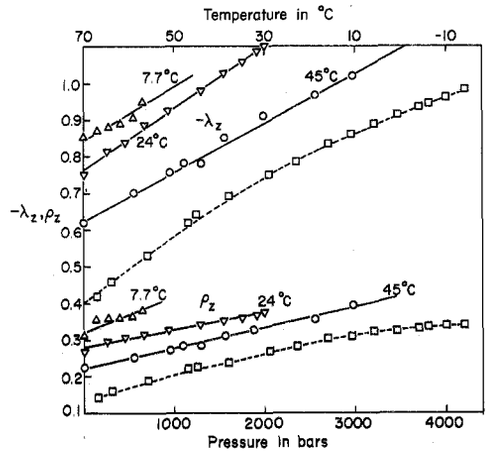

Figure 4. Asymmetric ordering, potential parameters, vs. pressure for PD-Tempone in phase V. The ordering parameters are defined with respect to the z molecular axis. The solid lines show least-squares fits. The dashed curve is for the temperature variation at 1 atm from Polnaszek and Freed.

"mean field" approaches are discussed in numerous places.[19-23] Note however the eq 3.5 for $U^{(s)}_{mf}$ assumes a spherically symmetric pair distribution function for simplicity, while for $U^{(p)}_{mf}$ this is not invoked to better allow for anisotropic ordering. The Maier-Saupe potential[19] is based on the assumption that only $\langle \boldsymbol{D}^{(2)(s)}_{00} \rangle$ is important and due to weak attractive forces, although more recent theories have included $\langle \boldsymbol{D}^{4(s)}_{00} \rangle$, but in different ways.[21,22] In general, for long rodlike solvents the K $\neq$ 0 terms in eq 3.5 should not be important, although for the probe they will generally have to be considered. While it is, in general, possible to represent all types of attractive and repulsive pairwise intermolecular forces by equations such as eq 3.5 and 3.6, some theories have introduced repulsive forces as a purely entropic, excluded volume between hard spheres.[10,20,24]

One general feature of the various theories is that each predicts a universal value for $S^{(s)} \equiv \langle \boldsymbol{D}^{2(s)}_{00} \rangle$ for the isotropic–nematic, and possibly for the nematic–solid phase transitions. NMR studies on the liquid crystal PAA as a function of T and P have confirmed this.[10] Our results at the nematic–solid phase transition for the different temperatures and pressures yield $S^{(p)}_{mp} = -0.14 \pm 0.017$, at the melting point. (However, there appears to be a definite trend such that $S^{(p)}_{mp}$ increases somewhat with increasing pressure.) This value is, as expected, smaller than the value 0.55 ± 0.015 obtained for $S^{(s)}_{mp}$ for PAA. Our results appear to indicate that the ordering of the probe is a definite monitor of the thermodynamic properties of the liquid crystalline solvent. Note that it has recently been shown that the presence of small amounts of impurities does not normally change the value of $S^{(s)}$ at the nematic–isotropic transition, and we may expect this to be true at the melting point as well.

The observed pressure dependence of the solid–nematic melting point for phase V is

$$T_{mp}(P) = -2.5\ °C + 12\ °C/kbar \times P \qquad (3.8)$$

(While substantial supercooling of the freezing point was noted in the temperature-dependent studies involving samples in thin capillary tubes, cf. I, it was not observed in this work.) This pressure dependence is smaller than that reported for PAA:[10]

$$T_{mp}(P) = 116\ °C + 24.5\ °C/kbar \times P \qquad (3.9)$$

Note that solutions of nematics with small amounts of impurity are known to be ideal, and they will cause a freezing point depression predicted in the usual fashion.

Our result can be interpreted, with the Clausius–Clapeyron equation (neglecting the small impurity effect) to yield at the melting point

$$\Delta H/\Delta V = T\left(\frac{dP}{dT}\right) = [T\,°\text{k})/12]\ \text{kbars} \qquad (3.10)$$

Unfortunately there is no latent heat (ΔH) or specific volume (ΔV) data available for phase V (or the similar MBBA solvent) at the melting point. [If we were to use the ΔV for PAA,[10,19] then we would get $\Delta H \sim 4.3$ kcal/mol.]

McColl[11] has introduced the thermodynamic quantity γ

$$\gamma \equiv \left(\frac{\partial \ln T}{\partial \ln \rho}\right)_S = -\left(\frac{\partial \ln T}{\partial \ln V}\right)_S \qquad (3.11)$$

as a measure of the relative importance of density (or specific volume) vs. temperature in establishing nematic order. This parameter is best calculated by converting data of $S^{(i)}$ taken as a function of T and P to results as a function of T and V by means of data on the T and P dependences of molar volume.[12] However, one may rearrange eq 3.11 for γ to obtain

$$\frac{1}{\gamma} = T\beta_T\left[\left(\frac{\partial P}{\partial T}\right)_S - \left(\frac{\partial P}{\partial T}\right)_\rho\right] \qquad (3.12)$$

where $\beta_T \equiv (\partial \ln \rho/\partial P)_T$ is the isothermal compressibility. Thus, while the slopes $(\partial P/\partial T)_S$ may be determined from our experiments, β_T and $(\partial P/\partial T)_\rho$ must be determined by other measurements. No such data have as yet been obtained for phase V, so we make use of published data on sonic velocity,[26] heat capacity,[27,28] and thermal expansion[29,30] for the liquid crystal MBBA, since in our previous work (I), we found that phase V and MBBA yielded similar results for ordering of the probe and for viscosity at the same temperatures. Our results for $(\partial P/\partial T)_S$ with some results on γ are given in Table I. Note that McColl and Shih[12] have found $\gamma = 4$, and it is constant over a range of temperatures (at 1 bar). Our estimates from less data amount to $\gamma \approx 1.9 \pm 0.4$. Note that this difference is directly traceable to our values of $(\partial P/\partial T)_S = 45$ bars/K, which is fairly constant, as shown in Figure 5 where nearly straight lines curves of T vs. P at constant $S^{(p)}$ have been obtained.[31] McColl[12] also found a near constancy, but with $(\partial P/\partial T)_S \simeq 23$ bars/K or nearly half our result. We also give results for another useful thermodynamic derivative, $(\partial S/\partial T)_V$, which may be obtained from our measurement, as was γ, using

$$\left(\frac{\partial S}{\partial T}\right)_V = \left(\frac{\partial S}{\partial T}\right)_P + \frac{\alpha}{\beta_T}\left(\frac{\partial S}{\partial P}\right)_T \qquad (3.13)$$

with $\alpha \equiv (\partial \ln V/\partial T)_P$ also computed from the published data.[26-30]

The theoretical importance of these quantities may be illustrated in the context of eq 3.5–3.7. The pair-interaction coefficients $u^{ij}_{L,K}(r_{ij})$ will in general depend on inverse powers of r_{ij} or r_{ij}^{-n}, e.g., $n = 6$ for dispersion forces which were the only forces introduced by Maier and Saupe.[19] More general treatments of attractive and repulsive forces yield more complex dependences on r_{ij}. One can hope to estimate a "mean" n from experiment to shed some light on the relative importance of these terms. This is done as follows. One *assumes* that

$$\bar{u}^{ij}_{L,K}(r_{ij}) \propto V^{-n/3} \qquad (3.14)$$

since an r_{ij}^{-n} dependence implies a $V^{-n/3}$ dependence. Now

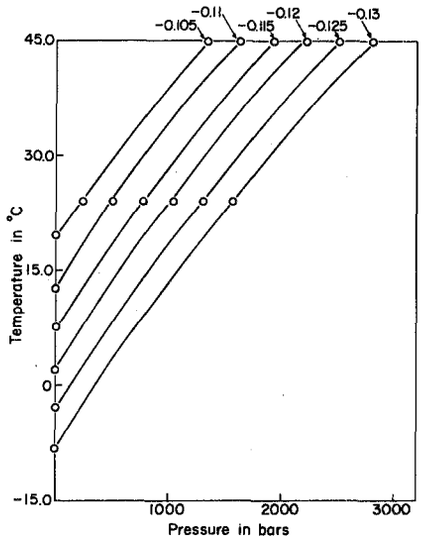

Figure 5. Graph of temperature vs. pressure showing contours of constant $\langle \boldsymbol{D}^{(2)}_{00} \rangle_z$. The results shown are for the pressure runs at 24 and 45 °C, and the atmospheric pressure experiments of Polnaszek and Freed (ref 5).

the minimization of the Helmholtz free energy of orientation in the limit of very dilute solution of probes, for the mean field potentials of eq 3.5 and 3.6 leads to the result that $P^{(s)}_{mf}(\Omega)$ is given by the form of eq 3.2, but with $U^{(s)}_{mf}$ given by eq 3.5. Then, in the mean field of the aligned solvent molecules, the distribution function for the probe molecules, $P^{(p)}_{mf}(\Omega)$, is also given by the form of eq 3.2, but with $U^{(p)}_{mf}$ of eq 3.6. Thus our measurements of $S^{(p)}$ are to be interpreted in the mean field theory by

$$S^{(p)} = \int \boldsymbol{D}^{2(p)}_{00}(\Omega) P^{(p)}_{mf}(\Omega)\, d\Omega \qquad (3.15)$$

Let us, purely for simplicity, assume Maier–Saupe-type potentials (i.e., only $\boldsymbol{D}^2_{00}(\Omega)$ terms in the expansions of eq 3.5 and 3.6). Furthermore we assume, $u^{sp}_2/kT = a^{sp}/V^{\gamma_p}T$ and $u^{ss}_2/kT = a^{ss}/V^{\gamma_s}T$ with a^{sp} and a^{ss} independent of T and V. Also a^{ss} is negative for rods and a^{sp} is positive for PD-Tempone. Then from the functional relation

$$S^{(i)}(T,V) = g_i(T,V,S^{(s)}) \qquad (3.16)$$

where i = s or p, (and, e.g., g_p is given by the right-hand side of eq 3.15) we obtain

$$\left(\frac{\partial S^{(i)}}{\partial T}\right)_V = \left(\frac{\partial g_i}{\partial S^{(s)}}\right)_{T,V}\left(\frac{\partial S^{(s)}}{\partial T}\right)_V + \left(\frac{\partial g_i}{\partial T}\right)_{S^{(s)},V} \qquad (3.17)$$

with a similar expression for $(\partial S^i/\partial V)_T$. We then obtain for this simple mean field model

$$\left(\frac{\partial \ln S^{(s)}}{\partial \ln T}\right)_V = \frac{(\Delta S^s)^2 a^{ss}/V^{\gamma_s}T}{1 + (\Delta S^s)^2 a^{ss}/V^{\gamma_s}T} \qquad (3.18)$$

where $(\Delta S^{(s)})^2$ is the mean square fluctuation in order parameter given by

$$(\Delta S^{(s)})^2 \equiv \langle (\boldsymbol{D}^{2(s)}_{00})^2 \rangle - \langle \boldsymbol{D}^{2(s)}_{00} \rangle^2 \qquad (3.19)$$

Then utilizing

$$\left(\frac{\partial T}{\partial V}\right)_{S^{(s)}} = -\left(\frac{\partial S^{(s)}}{\partial V}\right)_T \Big/ \left(\frac{\partial S^{(s)}}{\partial T}\right)_V \qquad (3.20)$$

we obtain

$$\left(\frac{\partial \ln T}{\partial \ln V}\right)_{S^{(s)}} = -\gamma_s \qquad (3.21)$$

TABLE I: Thermodynamic Quantities of PD-Tempone Dissolved in Phase V

					$(T/S^{(p)})(\partial S^{(p)}/\partial T)_V$	
T, K	$(\partial P/\partial T)_{S^{(p)}}$, mol/cm s^2 K	γ_p'	$S^{(p)}$	$S^{(s)}$ [a]	Exptl value	Predicted value from eq 3.22
298	1.68×10^5	2.28	−0.101	0.58	−1.85	−2.75
313	1.68×10^5	1.9	−0.0824	0.5	−2.58	−4.34

[a] The values given are for MBBA from ref 32.

Actually it is easy to show that eq 3.21 is obtained from more general mean field distribution functions utilizing eq 3.5, provided only that the $\bar{u}_{L,K}^{(ss)}/kT$ for all L and K show the same $1/V^{\gamma_s}T$ dependence; but eq 3.18 would then become more complicated. McColl and Shih[12] compare in a graph the Maier–Saupe prediction for $S^{(s)}$ vs. T at constant V with their actual experimental results. One sees that, in general, the $(\partial S^{(s)}/\partial T)_V$, which are *negative*, are predicted to be too large in magnitude by a Maier–Saupe theory. Note that $-(\Delta S^{(s)})^2 u^{ss}/kT$ is predicted from Maier–Saupe theory to range from ~1 to ¾ over the nematic range (with the values near unity in the vicinity of the isotropic–nematic phase transition). Thus, only small changes in the equivalent of $(\Delta S^s)^2 u^{ss}/kT$ resulting from including other terms in the potential (cf. eq 3.5, e.g., $\boldsymbol{D}_{00}^4(\Omega)$) will have a significant effect on the denominator of eq 3.18. Thus, we would expect that the equivalent of $(\Delta S^s)^2 u^{ss}/kT$ must be corrected to smaller values to agree with experiment by the inclusion of other terms in the potential.

The similar results for the probe ordering are given by

$$\left(\frac{\partial \ln S^{(p)}}{\partial \ln T}\right)_V = \frac{(\Delta S^{(p)})^2 a^{sp} S^{(s)}/V^{\gamma_p} T S^{(p)}}{1 + (\Delta S^{(s)})^2 a^{ss}/V^{\gamma_s} T} \tag{3.22}$$

and

$$-\left(\frac{\partial \ln T}{\partial \ln V}\right)_{S^{(p)}} = \gamma_p\left[1 + \frac{a^{ss}}{V^{\gamma_s} T}(\Delta S^s)^2\left(1 - \frac{\gamma_s}{\gamma_p}\right)\right] \tag{3.23}$$

where for PD-Tempone probe, $S^{(p)}$ is negative. Thus the mean field theory, wherein the ordering potential of the probe is taken to be proportional to $S^{(s)}$ (cf. eq 3.6), aptly shows from eq 3.23 that the volume dependence at constant $S^{(p)}$ depends on both γ_p and γ_s. And, in general, the thermodynamic dependence of $S^{(p)}$ is a function of both u^{sp} and u^{ss}. We list, in Table I, the results for $(\partial \ln S^{(p)}/\partial \ln T)_V$ predicted from eq 3.22 from our measurements on $S^{(p)}$ and published results on MBBA[32] for $S^{(s)}$ (recall that the results in I implied very similar ordering behavior in MBBA and phase V). These predictions are qualitatively in reasonable agreement with the experimental values, but tend to be 50–70% high. However, our previous discussion of $(\partial \ln S^{(s)}/\partial \ln T)_V$ indicated that a "corrected" $(\Delta S^{(s)})^2 u^{ss}/kT$ that is smaller than the prediction from a Maier–Saupe potential is needed to produce agreement with experiment. This also clearly applies to eq 3.22, and the order of the correction in this parameter (i.e., about 25% lower) is also similar. Thus, the thermodynamic properties of the probe ordering $S^{(p)}$ appear to be amenable to the same kind of analysis as $S^{(s)}$. The expression of eq 3.23 suggests that our measurement of γ (call it γ_p') is roughly $\gamma_p' \sim (\frac{1}{4}\gamma_p + \frac{3}{4}\gamma_s)$, for $(\Delta S^{(s)})^2 u^{ss}/kT \sim -\frac{3}{4}$, but with a "corrected" $(\Delta S^{(s)})^2 u^{ss}/kT$, it would, from the above indications, be closer to $\gamma_p' \sim \frac{1}{2}(\gamma_p + \gamma_s)$. Thus, it may well be that our result of $\gamma_p' \sim 2$ compared to McColl's $\gamma_s = 4$ in PAA reflects either a $\gamma_p < \gamma_s$ in phase V (or "quasi"-MBBA) or else if $\gamma_p = \gamma_s$ in this solvent, then the overall result is different from PAA. Note, however, that our observed trend of $S_{mp}^{(p)}$, viz., that it appears to show a systematic increase with increasing P_{mp} would in the context of the mean-field theory used here, imply $\gamma_p < \gamma_s$, provided $S_{mp}^{(s)}$ is constant as one expects.[10]

4. Relaxation and Rotational Reorientation

(A) *Line Width Analysis. Motional Narrowing Region.* The observed motional narrowing line widths are fit to the usual quadratic in m_I, the z component of the ^{14}N nuclear spin quantum number:

$$T_2^{-1}(m_I) = A + Bm_I + Cm_I^2 \tag{4.1}$$

The results for the variation of A, B, and C plotted logarithmically with pressure are shown in Figure 6. The ln A, ln B, and ln C are found to be linear with pressure except for the higher pressures consistent with the onset of slow tumbling. The results are found to be very similar to the results in I obtained as a function of T. The overall similarity in results for the different pressures and the work of I is emphasized in Figure 7 where the important C/B ratio[2-5] is plotted vs. τ_R (the determination of τ_R, the rotational correlation time, is discussed below). The increase in C/B with τ_R is due to some extent to the increase in ordering as either the pressure is raised or the temperature is lowered. (For an isotropic liquid C/B should remain constant.) However, there is a substantial increase in C/B with τ_R not attributable to the ordering. As in I, this may be interpreted in terms of (1) anisotropic viscosity; (2) anisotropic diffusion; (3) modification of the pseudo-secular spectral densities to

$$j(\omega_a) = \frac{\tau_R}{1 + \epsilon'\omega_a^2\tau_R^2} \tag{4.2}$$

where, for $\epsilon' = 1$, one recovers the well-known Debye spectral density. We summarize these (and other) mechanisms in Table II. None of these explanations are really satisfactory, and again for the same reason given in I. We summarize some of these reasons. When the results are analyzed in terms of anisotropic viscosity, the value of $\hat{N} \equiv \hat{\tau}_{R_\perp}/\hat{\tau}_{R_\parallel}$ continues to increase with increasing $\hat{\tau}_{R_\perp}$ (i.e., $\hat{\tau}_{R_\parallel}$ remains nearly equal while $\hat{\tau}_{R_\perp}$ increases considerably). [Here $\hat{\tau}_{R_\perp}$ and $\hat{\tau}_{R_\parallel}$ are the components of the rotational correlation time that are respectively perpendicular and parallel to the director.] When the results are analyzed in terms of anisotropic diffusion, one finds that $N_y \equiv \tau_{R_\perp}/\tau_{R_\parallel}$ must be increasing as $\tau_{R_\perp}$ increases, and this is "turned on" only for $\tau_{R_\perp} > 2 \times 10^{-10}$ s. Furthermore, when $\tau_R \gtrsim 10^{-9}$ s, A' is predicted to be negative. This is totally unexpected; typically A' is found to increase with increasing τ_R.[2-5] [Here $\tau_{R_\perp}$ and $\tau_{R_\parallel}$ are referred to a symmetry axis of the molecule.] The modification of the pseudo-secular spectral density with $\epsilon' \sim 13$–20 yields results for τ_R equal to that of the values of $\hat{\tau}_{R_\perp}$ for the anisotropic viscosity model. However, in this case, a single, constant parameter (viz., ϵ') adequately explains a range of results. [More precisely $\epsilon_{ps} \approx$

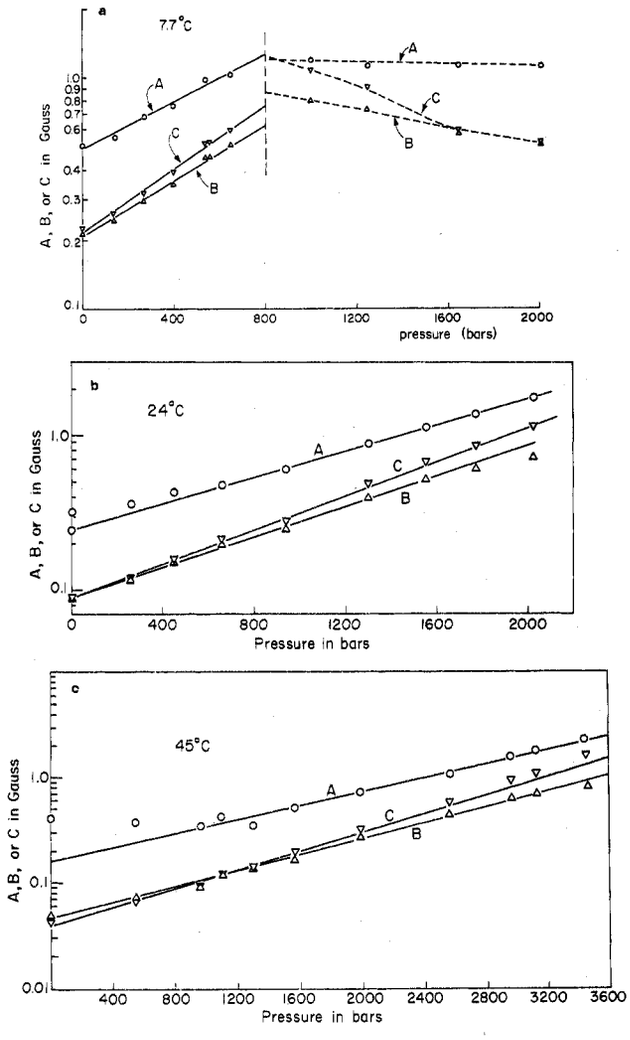

Figure 6. Line width parameters A, B, or C from fit of line width to expression $A + BM_N + CM_N^2$ (where M_N is the ^{14}N nuclear spin quantum number) plotted vs. pressure. The solid lines are the least-square fits. Parts a, b, and c are respectively for 7.7, 24, and 45 °C. The dashed lines in part a are results for the solid phase; the phase transition is indicated by the vertical dashed line.

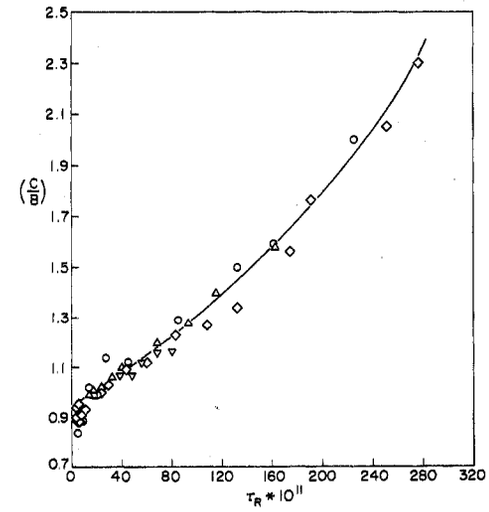

Figure 7. Graph of (C/B) vs. τ_R for PD-Tempone in phase V. The points marked by O, Δ, and ∇ are for 45, 24, and for 7.7 °C, respectively. The points marked ◇ are for the temperature variation at 1 atm from Polnaszek and Freed.[5]

20 effectively "explains" the low temperature lower pressure results, while $\epsilon'_{ps} \approx 13$ is better for the higher temperature, high pressure results.] Thus the analysis in terms of ϵ' is a useful way of representing the data and, as discussed in I and in Section C below, it has certain theoretical implications. Its limitations will be discussed below.

The results of an analysis of C and B to yield τ_R for the different models according to the procedures in I are given in Figure 8. That is, the analysis was based on the appropriate diffusion solutions under the two-term potential, eq 3.3, with the values of λ_z and ρ_z given in Figure 4. The theoretical expressions for the line widths $(A - A')$, B, and C are given by eq 2.31 of I, and computer programs for their computation are given elsewhere.[33] It is seen from Figure 8 that the actual results for τ_R are not very sensitive to the particular model (no more than 10% difference). Since the anomalies, presumably due to model-dependent effects, become much greater in the slow-motional region, we defer further discussion of this.

(B) *Activation Energy and Volume.* The variation of τ_R with pressure at 8, 24, and 45 °C is shown in Figure 8. One finds that ln τ_R is linear in P (as well as in $1/T$). It is possible to obtain the usual activation enthalpies ΔH_a and volumes ΔV_a from the P and T dependences, respectively.[7,8,34,35a] That is, if we assume activated-state theory for convenience, we may write

$$\tau_R = \tau_{R,0} \exp[\Delta G_a/RT] \tag{4.3}$$

where ΔG_a is the difference in Gibbs function between the initial and the activated state. One expects $\tau_{R,0}$ to be almost T and P independent, and we assume that it is. Then, from the thermodynamic relations

$$\Delta G_a = \Delta H_a + T(\partial \Delta G_a/\partial T)_P = \Delta H_a - T\Delta S_a \tag{4.4}$$

and

$$\Delta V_a = (\partial \Delta G_a/\partial P)_T \tag{4.5}$$

one easily finds that

$$\Delta H_a = R\left[\frac{\partial \ln \tau_R}{\partial(1/T)}\right]_P = -RT^2\left[\frac{\partial \ln \tau_R}{\partial T}\right]_P \tag{4.6}$$

and

$$\Delta V_a = RT\left(\frac{\partial \ln \tau_R}{\partial P}\right)_T \tag{4.7}$$

respectively. Our data analyzed in this way yield

$$\Delta H_a = (9.37 + 0.001\ 02P)\ \text{kcal/mol} \tag{4.8}$$

with P in bars (e.g., ΔH_a is 9.43, 9.55, 10.28, 10.92 kcal/mol for P = 1, 200, 1000, and 1500 bars, respectively). [The linear variation of ln τ_R with $1/T$ results in a temperature independent ΔH_a.] Also

$$\Delta V_a = (53.7 - 0.079T)\ \text{cm}^3\text{/mol} \tag{4.9}$$

and T is in K (i.e., ΔV_a is 31.3, 30.4, 28.5 cm^3/mol for T = 281, 297, 318 K, respectively). [The linear variation of ln τ_R with P results in a pressure independent ΔV_a.] By analogy to eq 4.6 one typically defines

$$\Delta E_{V,a} \equiv R\left[\frac{\partial \ln \tau_R}{\partial(1/T)}\right]_V \tag{4.10}$$

Then, since

$$\left(\frac{\partial \Delta G_a}{\partial T}\right)_V = -\Delta S_a + \left(\frac{\partial P}{\partial T}\right)_V \Delta V_a \tag{4.11}$$

one easily shows that

TABLE II: Summary of Rotational Relaxation Mechanisms

Mechanism	Characteristic	Parameters	Ref
(1) Anisotropic diffusion	Unequal reorientation rates about principal axis system fixed in molecule. When the reorientation rates are equal this becomes isotropic Brownian rotational diffusion.	$R_\parallel = (6\tau_{R_\parallel})^{-1}$ rotational diffusion coefficient about molecular symmetry axis. $R_\perp = (6\tau_{R_\perp})^{-1}$ rotational diffusion coefficient about molecular axes perpendicular to symmetry axis. $N = \tau_{R_\perp}/\tau_{R_\parallel}$	2a; J. H. Freed, *J. Chem. Phys.*, **41**, 2077 (1964)
(2) Anisotropic viscosity	Unequal reorientation rates about principal axis system fixed in the laboratory (e.g., dc magnetic field axis).	$\hat{R}_\parallel = (6\hat{\tau}_{R_\parallel})^{-1}$ rotational diffusion coefficient about orienting axis in lab frame. $\hat{R}_\perp = (6\hat{\tau}_{R_\perp})^{-1}$ rotational diffusion coefficient perpendicular to orienting axis in lab frame. $\hat{N} = \hat{\tau}_{R_\perp}/\hat{\tau}_{R_\parallel}$	4; 5; C. F. Polnaszek, G. V. Bruno, and J. H. Freed, *J. Chem. Phys.*, **58**, 3185 (1973)
(3) Fluctuating torques	Anisotropic torques which induce reorientation are themselves relaxing at a rate that is not much faster than the reorientation of the probe molecule.	τ_R = relaxation time for rotational diffusion of probe molecule. τ_M = relaxation time for fluctuating torques inducing reorientation of probe molecule. $\epsilon' \equiv (1 + \tau_M/\tau_R)^2$. May be combined with analogues of models 1 (requiring additional specification of $\tau_{M\parallel}$ and $\tau_{M\perp}$) or 2 (requiring $\hat{\tau}_{M\parallel}$ and $\hat{\tau}_{M\perp}$).	3; 18
(4) SRLS	Probe molecule relaxes in a local potential field, while the latter averages out isotropically at a significantly slower rate than the rate of probe molecule reorientation.	$S_1 = \frac{1}{2}\langle 3\cos^2\theta - 1\rangle$ the order parameter of the probe relative to the local anisotropic potential field (i.e., local structure). This ordering is assumed to be cylindrically symmetric for simplicity. τ_x = the relaxation rate of the local structure. (May also be combined with the analogues of models 1 or 2.)	5
(5) Jump diffusion	Molecule reorients by random jumps of arbitrary angle.	$R = (\epsilon^2)_{av}/6\tau$ where τ is the time between jumps and $(\epsilon^2)_{av}$ is the mean-square jump angle. Can be generalized to include anisotropic diffusion tensors, by analogy with models 1 or 2.	2a
(6) Free diffusion	Molecular reorientation is partially due to free gaslike motion which is perturbed by the frictional effects of the surroundings.	τ_R and τ_J where τ_J is the angular-momentum relaxation time. They are often related by the Hubbard–Einstein relation: $\tau_R\tau_J = I/6kT$ with I the moment of inertia. Also $\tau_J^{-1} = \beta$ the friction coefficient.	2a; 3; G. V. Bruno and J. H. Freed, *J. Phys. Chem.*, **78**, 935 (1974).
(7) Director fluctuations	A hydrodynamic effect in which the nematic director fluctuates in its orientation with respect to the applied magnetic field.	$\tau_q^{-1} = K_q^2/\eta$ where τ_q is the relaxation time of the qth Fourier component of the director fluctuation, with K the average elastic constant of the liquid crystal and η is the viscosity.	5

$$\Delta E_{V,a} = \Delta H_a - T\left(\frac{\partial P}{\partial T}\right)_V \Delta V_a \qquad (4.12)$$

The partial derivative $(\partial P/\partial T)_V = \alpha/\beta$ where $\alpha \equiv (1/V)(\partial V/\partial T)_P$ and $\beta \equiv -(1/V)(\partial V/\partial P)_T$ have already been used in section 3. We have estimated α and β from the appropriate data on MBBA (cf. section 3) to obtain

$$\Delta E_{V,a} \approx 0.803 + 0.001\,02P + 0.0126T \text{ kcal/mol} \qquad (4.13)$$

which is applicable only for $T \simeq 313$ K and $P \sim 1$ bar. To the extent that one accepts activated state theory, ΔH_a and $\Delta E_{V,a}$ are measures of the energy required to reorient a molecule under conditions of constant P and V, respectively. Then eq 4.8, 4.9, and 4.13 are consistent with the intuitive picture[35a] that (1) the restoring torques exerted on the probe (hence ΔH_a) increase as P increases, since the free volume is reduced; and (2) the kinetic molecular fluctuations increase as T increases so the activation volume that is needed decreases. The T and P dependence of $\Delta E_{V,a}$ is then a composite of these reasons, cf. eq 4.12.

(C) *Slow Motional Region and the Various Reorientational Models.* Typical spectra obtained at the highest pressures for which the nematic solvent has not frozen are shown in Figures 9–11. The largest values of τ_R occurred, surprisingly enough, at the higher temperatures, as a result of the nature of the pressure dependence of the phase transition (cf. eq 3.8) vs. the activation free energy of τ_R (cf. eq 4.3, 4.6–4.9). Also shown in those figures are the theoretical spectra predicted for an isotropic Brownian motion model with the λ_z and ρ_z from Figure 4, and the τ_R's from Figure 8 (extrapolated where necessary).

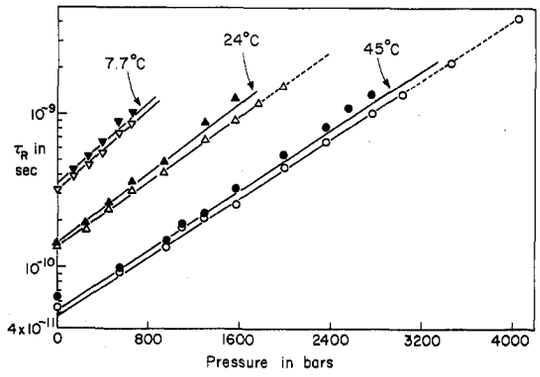

Figure 8. Graph of τ_R vs. pressure for PD-Tempone in phase V. The best fits with an asymmetric potential (i.e., either anisotropic viscosity or $\epsilon' \neq 1$) are shown by ∇, △, ○, while the best fits with an anisotropic rotation model are shown by ▼, ■, ●. See text. The dashed lines represent extrapolated values used for the slow tumbling simulations.

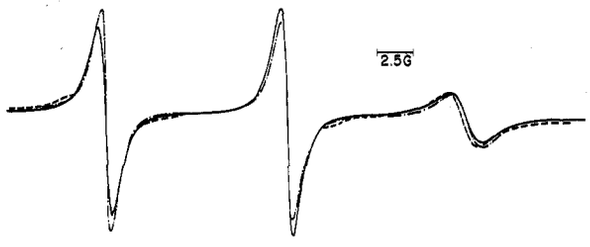

Figure 9. Comparison of experimental and simulated spectra at 7.7 °C and 652 bars for PD-Tempone in phase V: (- - - -) experimental result; (– O – O –) theoretical result based on isotropic Brownian diffusion with $\tau_R = 8.0 \times 10^{-10}$ s, $\lambda_z = -0.945$, $\rho_z = 0.38$, and $A' = 1.18$ G; (—) theoretical result based upon model with $\epsilon_s' = 1$, $\epsilon_{ps}' = 20$, $A' = 0.33$ G but other values given by the Brownian model.

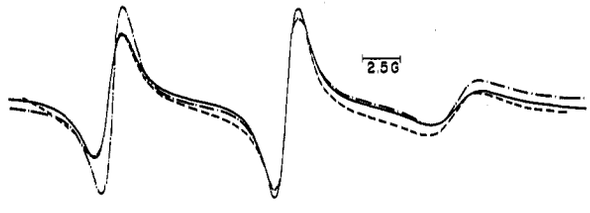

Figure 10. Comparison of experimental and simulated spectra at 24 °C and 1974 bars for PD-Tempone in phase V: (- - - -) experimental result; (– O – O –) theoretical result based on isotropic Brownian diffusion with $\tau_R = 1.59 \times 10^{-9}$ s, $\lambda_z = -1.096$, $\rho_z = 0.37$, and $A' = 0.12$ G; (—) theoretical result based upon model with $\epsilon_s' = 1$, $\epsilon_{ps}' = 13$, $A' = 0.52$ G, but other values given by the Brownian model.

It is clear that there are large discrepancies between experimental and predicted spectra, and they become worse as τ_R increases. These discrepancies are virtually the same as was observed in I for temperature-dependent studies. As in I, it was possible to get satisfactory fits with the anisotropic viscosity model but with anomalously large values of $\tilde{N}$ (and with $\hat{\tau}_{R\parallel}$ eventually having to become negative for the slower motions). The anisotropic diffusion model is not satisfactory and it requires that A' become negative.

As in I, it was possible to satisfactorily fit the spectra with a model based upon frequency-dependent diffusion coefficients, which result from having fluctuating intermolecular torques that induce the reorientation but are not fluctuating at a rate which is much faster than the reorientation. However, it was again necessary to distinguish between components which are parallel and perpendicular to the director. This

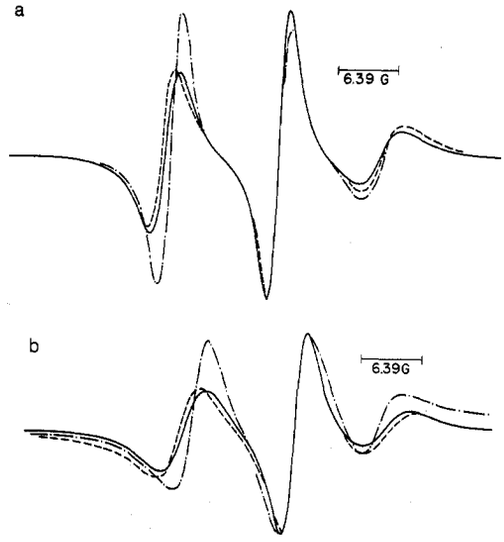

Figure 11. Comparison of experimental and simulated spectra at 45 °C for PD-Tempone in phase V: (a) 3450 bars, (- - - -) experimental result; (– O – O –) theoretical result based on isotropic Brownian diffusion with $\tau_R = 2.25 \times 10^{-9}$ s, $\lambda_z = 1.124$, $\rho_z = 0.40$, and $A' = 0$; (—) theoretical result based upon model with $\epsilon_s' = 1$, $\epsilon_{ps}' = 13$, and $A' = 0.95$ G, but other values given by the Brownian model; (b) 4031 bars, (- - - -) experimental result; (- O - O - O -) theoretical result based on isotropic Brownian diffusion with $\tau_R = 4.3 \times 10^{-9}$ s, $\lambda_z = -1.21$, $\rho_z = 0.43$, and $A' = 0$; (—) theoretical result based upon model with $\epsilon_s' = 1$, $\epsilon_{ps}' = 13$, and $A' = 1.35$ G but other values given by the Brownian model.

matter is discussed in more detail in I. Here we just note the simplified formulae in the limit of zero ordering for L = 2:

$$j_{2,s}(\omega) = \hat{\tau}_{R\perp}/[1 + \epsilon_s'\hat{\tau}_{R\perp}\omega^2] \tag{4.14a}$$

$$\epsilon_s' = (1 + \hat{\tau}_{M\perp}/\hat{\tau}_{R\perp})^2 \tag{4.14b}$$

and

$$j_{2,ps}(\omega) = \hat{\tau}_{R,1}/[1 + \epsilon_{ps}'\hat{\tau}_{R,1}\omega^2] \tag{4.15a}$$

$$6\hat{\tau}_{R,1}^{-1} = 5\hat{\tau}_{R\perp}^{-1} + \hat{\tau}_{R\parallel}^{-1} \tag{4.15b}$$

and

$$\epsilon_{ps}' = \left(1 + \frac{5}{6}\hat{\tau}_{M\perp}/\hat{\tau}_{R\perp} + \frac{1}{6}\hat{\tau}_{M\parallel}/\hat{\tau}_{R\parallel}\right)^2 \tag{4.15c}$$

In these expressions $\hat{\tau}_{M\perp}$ and $\hat{\tau}_{M\parallel}$ are the relaxation times for the fluctuating torques inducing the reorientation, i.e., for those components parallel and perpendicular to the director. The subscripts s and ps refer to secular and pseudo-secular (or nuclear-spin flip) contributions, respectively.[5] In general, we require $\epsilon_s' \sim 1$ or 2 and $\epsilon_{ps}' \sim 20$ for low T and low P slow tumbling while $\epsilon_{ps}' \sim 13$ for high T and high P slow tumbling. These results are consistent with the motional narrowing analysis, but they are more dramatic in the slow tumbling case. This is evidenced in Figures 9–11, where the results of such an analysis are presented.[35b]

We have carried out an analogous analysis in terms of anisotropic fluctuating torques referred to the molecular, as opposed to the director frame. Here one specifies $\tau_{R\parallel}$, $\tau_{R\perp}$, $\tau_{M\parallel}$, and $\tau_{M\perp}$, and one obtains expressions analogous to (but different from) those for the director frame. However, we could find no set of values of the adjustable parameters which could yield predictions in satisfactory agreement with experiment.

Despite the fact that the analysis based upon fluctuating

torques as described above and shown in Figures 9–11 yielded satisfactory agreement with experiment, it was argued in I that such large values of ϵ_{ps}' are inconsistent with the physical model; i.e., it implies $\hat{\tau}_{M\parallel} \gg \hat{\tau}_{R\parallel}$. Thus another model was considered there, viz., one assumes that significant components of the fluctuating torque persist for times long compare to τ_R. Then, on a longer time scale, τ_X, these components relax isotropically or nearly isotropically. This "slowly relaxing local structure" (SRLS) mechanism was analyzed in I and approximate expressions were given for their contribution to the line width. These comments also apply to our present results. The SRLS is an effective mechanism for explaining an anomalous increase in C/B. Order of magnitude estimates yield $S_1^2 \equiv \langle \boldsymbol{D}_{00}^2(\Omega) \rangle_1 \sim 1/16$, where S_1 measures the ordering of the probe relative to the temporarily static torque components, while $\tau_X/\tau_R \sim 10$. In particular, for motionally narrowed spectra, and where S_1 is not large, one can derive expressions for the spectral densities $j_0(\omega)$ and $j_2(\omega)$

$$j_0(\omega) = \frac{\tau(0)}{1 + \omega^2\tau(0)^2} \rightarrow \left[D_0(\omega) + \frac{S_1^2\tau_X}{1 + \omega^2\tau_X^2} \right] \quad (4.16a)$$

$$j_2(\omega) = \frac{\tau(2)}{1 + \omega^2\tau(2)^2} \rightarrow D_2(\omega) \quad (4.16b)$$

where the first equality is the usual definition of the spectral density for anisotropic diffusion in an isotropic liquid[2] and the arrow points to the new result.[36] Also the $D_0(\omega)$ and $D_2(\omega)$ are given in I, and for $\omega\tau(0)$, $\omega\tau(2) \ll 1$, and $S_1 \lesssim 0.8$ one has (using a more accurate expansion than in I):

$$D_0(\omega = 0) \simeq [1 + 0.27S_1 - 2.87S_1^2 + 1.522S_1^3]\tau(0) \quad (4.17a)$$

$$D_2(\omega = 0) \simeq [1 + 0.052S_1 + 0.264S_1^2 + 0.177S_1^3]\tau(2) \quad (4.17b)$$

while for negative $S_1 \gtrsim -0.4$ one has

$$D_0(\omega = 0) \simeq [1 - 0.180S_1 - 3.11S_1^2 - 6.34S_1^3]\tau(0) \quad (4.18a)$$

$$D_2(\omega = 0) \simeq [1 - 0.134S_1 - 0.601S_1^2 - 2.654S_1^3]\tau(2) \quad (4.18b)$$

As in I, we assume that the molecular magnetic z axis orients perpendicular relative to the local ordering, so eq 4.18 apply. Then the hyperfine tensor is very nearly axially symmetric in this molecular reference frame, so at X-band we can neglect in a first approximation the terms contributing to A, B, and C from $D_2(\omega)$. Then for our rough estimates of $S_1^2 \sim 1/16$ and $\tau_X/\tau_R \sim 10$, the terms $D_0(\omega)$ and $S_1^2\tau_X/[1 + \omega^2\tau_X^2]$ contribute roughly comparably for $\omega^2\tau_X^2 \ll 1$ (more precisely $D_0(0) \sim 0.95\tau(0)$ and $S_1^2\tau_X \sim 0.6\tau(0)$, while for $S_1^2 \sim 0.1$, $D_0(0) \sim 0.8\tau(0)$ and $S_1^2\tau_X \sim \tau(0)$). Thus, this analysis indicates that τ_R calculated from $j_0(\omega)$ might be about 60% larger than the true value. (We have not attempted a total reanalysis based on such an observation given the other approximations in our analysis.)

One can explain the anomalous part of the C/B increase which begins to develop for $\tau_R > 2 \times 10^{-10}$ s by the choice of $\tau_X/\tau_R \sim 10$. This requires the analysis of the SRLS mechanism for $\tau_X > 2 \times 10^{-9}$ s, which is near the incipient slow-motional region for nitroxides. However, the analysis of A, B, and C near the incipient slow motional region becomes complicated because of the need to precisely distinguish the relevant secular and pseudo-secular frequencies for the spectral densities associated with the $S_1^2\tau_X/[1 + \omega^2\tau_X^2]$ term. The more complex calculations which are required are summarized elsewhere.[4,5,33] We show in Figure 12, the results of the contributions to A, B, and C from the SRLS mechanism, which were only briefly summarized in I. It should be emphasized that these results have been calculated neglecting any effects from the actual mean potential (cf. eq 3.3), so one must analyze the results assuming additivity of its effects with that of the SRLS mechanism. Note that the increase in C/B is indeed predicted for $\tau_X > 2 \times 10^{-9}$ s from this contribution to the width, and it becomes very dramatic for $\tau_X \sim 10^{-8}$ s, corresponding to $\tau_R \sim 10^{-9}$ s (according to our analysis) and this is indeed consistent with our experimental observations both in I and in the present work. Since a careful analysis based upon slow tumbling becomes important for $\tau_X \gtrsim 2.5 \times 10^{-9}/S_1$ (or $\sim 2.5 \times 10^{-8}$ s in the present case) the results shown in Figure 12 should not be used for the slower values of τ_X. It is seen from results quoted in I that more dramatic effects may be obtained, hence smaller values of S_1^2 and/or τ_X/τ_R would be needed, if there is substantial anisotropy in the relaxation of the local structure. Furthermore, one would expect S_1^2 to increase somewhat as the temperature is lowered and the pressure is increased.

Clearly, it is somewhat arbitrary to distinguish models in which the fluctuating torques are relaxing at rates comparable to or significantly greater than the reorienting probe molecule. Fluctuating torque components must be relaxing over a very wide range of frequencies.[37] However it seems reasonable that, for a small spherical probe in a solvent of long rodlike nematic solvent molecules, there will indeed exist local structure around the probe, which can relax only by the more improbable reorientation of the solvent molecules about axes perpendicular to the director (however, for typical values of $S^{(s)} \sim 0.35$–0.55; the Maier–Saupe-type theory prediction is $(\Delta S^{(s)})^2 \sim 0.2$–$0.15$ roughly corresponding to root-mean square angular fluctuations of ~ 37–$40°$; however, the actual values are probably somewhat smaller, cf. section 3). Or, perhaps even more likely, the translational diffusion of the rodlike solvent molecules directly affects the local structure about the probe.

We have discussed in I the de Gennes–Pincus-type hydrodynamic model for fluctuations in the director[38] and its potential effect on ESR relaxation.[5] There it was concluded that it was both qualitatively and quantitatively of the wrong character to explain the observed anomalies. Our pressure-dependent results reinforce these conclusions. It is perhaps useful to distinguish between the two models or mechanisms: SRLS, and hydrodynamic director fluctuations. In simple physical terms, the former is a model involving molecular dimensions and molecular diffusion, while the latter involves coupled modes or waves with dimensions much greater than molecular dimensions. Partly as a result of this, the rotational reorientation of the probe molecule should be more significantly affected by the former molecular-type process. The frequency and temperature dependence of the latter model has been worked out,[38,39] and it is substantially different from that for molecular reorientation. Our combined temperature and pressure studies show that the relaxation anomalies are closely related in their T and P dependence to the rotational reorientation, τ_R, while τ_R exhibits very similar activation energies as the twist viscosity of the liquid crystal (cf. I). It is reasonable to expect that the SRLS mechanism is closely coupled to the rotational and translational diffusion processes of the solvent molecules. The frequency dependence of such a mechanism has not been analyzed yet; the discussion above

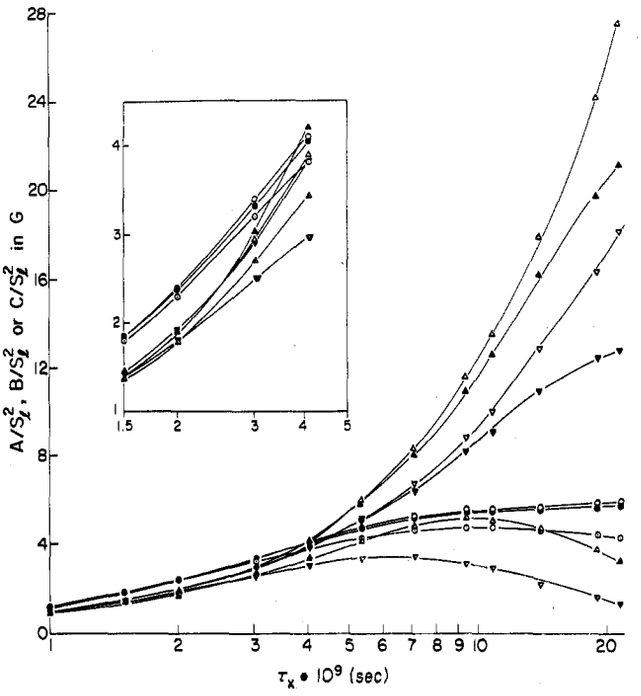

Figure 12. Graph of the contributions of the slowly relaxing local structure (SRLS) mechanism to the nitroxide line widths as a function of τ_X, the relaxation time for the local structure. The results are given as A/S_l^2, B/S_l^2, C/S_l^2, where S_l is the local structure order parameter, and these are the additional contributions to be added to the main contributions due to the overall molecular reorientation. The O, ●, ⊙ are the A/S_l^2 values for S_l = ⅛, ¼, and 1, respectively; the ▽, ▼, ▽ are the B/S_l^2 values for S_l = ⅛, ¼, and 1, respectively; and the △, ▲, ◬ are the C/S_l^2 values for S_l = ⅛, ¼, and 1, respectively. The insert shows a portion of the main graph on an expanded scale.

assumes a simple Debye-type spectrum from the relaxing local structure. The qualitative effects of the two mechanisms on ESR relaxation (i.e., the relative magnitudes *and* signs of the contributions to A, B, and C) need not necessarily be different. For the analysis yielding Figure 12, it is assumed that the local structure about the probe is distributed isotropically; i.e., one averages the persistent local torque over an isotropic distribution. This is not at all unreasonable for a spherical probe weakly ordered in the liquid crystal. The director fluctuation model is not isotropic in this sense. The director fluctuations are small increments from the mean director. [One could, of course, incorporate such a feature into the local structure mechanism, as was shown in I.] Because of this feature, it is predicted to make just a pseudo-secular (and nonsecular, or $M = \pm 1$ terms in general) contribution to the ESR, A, B, and C terms. In particular it would reduce C, hence C/B, which is opposite to the observed effect. An isotropic model can contribute just as effectively to secular ($M = 0$) and pseudo-secular ($M = \pm 1$) terms, and, as shown in Figure 12, lead to an *increase* in C/B for appropriate values of τ_X.

Our analysis of the SRLS mechanism on the ESR line shapes is still very approximate, and the complicating features of slow tumbling in τ_R and τ_X have not as yet been adequately dealt with, although the methods have been outlined in I. This is, in part, why the theoretical fits of the incipient and slow tumbling spectra in Figures 9–11 have been based mainly on the probably less important frequency-dependent diffusion model (or mechanism). It represents, nevertheless, an effective "semiempirical" method for fitting our results.

We turn now to what appears to be a somewhat larger effect ($\epsilon' \sim 20$) at low T and P compared to high T and P ($\epsilon' \sim 13$). In the context of the activation analysis of the previous section, this would imply that the increase in the local structure (or restoring torques), due to the reduction in free volume as P is increased, is somewhat more than offset by the effects of the kinetic molecular fluctuations as T increases, which permits larger fluctuations of the probe, hence reduced ordering with respect to the local structure, as well as more rapid relaxation.

(D) *Frozen Solutions.* When the pressure is increased above the values at the freezing point (shown in Figure 3), a metastable form of phase V is observed. The motion of the spin probe slows down considerably. This metastable form decays to a stable solid within about 10 min. Because of this rapid change, we were not able to obtain well-defined reproducible spectra for possible simulation.[40]

The spectrum of PD-Tempone in the solid phase is like that in isotropic liquids in the motional narrowing region, i.e., there are three fairly sharp unshifted lines. It was noted in I, where the frozen solutions yielded ESR spectra characteristic of the rigid limit, that these spectra showed no preferential ordering. Line width parameters for this frozen phase are displayed in Figure 6a. One notes (1) that B and C appear to change discontinuously at the freezing point and (2) that B and C are *decreasing* as the pressure is increased above its value at the freezing point. Observation (1) requires some explanation. Our theoretical estimates are that ordering potentials typical of PD-Tempone in the nematic phase should lead to values of B and C that are about 30% lower than for the isotropic phase, provided τ_R remains the same. The isotropic and nematic values of B, when extrapolated to the freezing point, actually do lead to comparable estimates of τ_R (1.0×10^{-9} and 9.1×10^{-10} s for the nematic and isotropic phases, respectively). Now observation (2) implies that τ_R decreases as the pressure is increased in the solid phase, as though the probe is located in a cavity (or clathrate) and, from the estimates of τ_R from B, this structure is like that in the nematic phase, except that increasing the pressure freezes out movement of solvent molecules, and the motion of the spin probe becomes less hindered. At still higher pressures, the free volume of the cavity should be reduced, and τ_R should again increase.[41]

We have not yet considered the increase in C upon freezing, which is larger than expected from the change in B discussed above. In the context of the SRLS mechanism, one notes from Figure 12 that an enhanced C/B ratio results from its large relative contributions to C. If the local structure is relaxing more slowly, i.e., τ_x is longer in the solid phase, and/or S_l becomes larger, then one might expect an enhanced C/B ratio. However, in our analysis of SRLS, we have assumed that in the nematic phase, its effects and those of the macroscopic director are additive. This may not be true, so we cannot at present be confident of the proposed explanation for the large increase in C upon freezing. Note, however, that when the pressure has been increased substantially (and τ_R has decreased) in the solid phase, then $C/B \approx 1$, which is expected if the SRLS is not important.

5. Conclusions

In this work, it was shown that pressure-dependent ESR studies can supply useful information about molecular ordering and dynamics in liquid crystalline solvents. The results on molecular ordering could be discussed in terms of simple mean field theory to show how they reflect, in general, the combined effects of the orientation dependent interactions between solvent molecules as well as between solvent and

probe. The present results for a spherical probe molecule are consistent with somewhat longer range interactions ($\gamma_P' = 1.9 \pm 0.4$) than the results of McColl on a pure solvent (PAA with $\gamma_s = 4.0 \pm 0.1$), although the present results are somewhat of a preliminary nature.

The pressure-dependent spin-relaxation studies both amplify and support the previous temperature-dependent studies on this system, and the results have been subjected to an activated state theory analysis. The anomalous relaxation behavior previously noted for the temperature-dependent studies in the incipient slow-tumbling region has been confirmed as a function of pressure. It is shown that this anomalous behavior is nearly independent of what combination of T and P is required to achieve a given τ_R. The strong dependence of the anomaly on τ_R, and its virtual independence of the particular combination of T and P, is taken as strong evidence that the anomalous behavior is directly related to the *viscous* modes of motion associated with the reorientation of the spin probe in its surroundings of rodlike molecules. It has been argued that the most likely explanation for the anomaly is a slowly relaxing local structure mechanism, in which the rodlike solvent molecules present a persistent local structure for the probe, which relaxes on a time scale much slower than the reorientation of the probe. Furthermore, this would be consistent with an apparent cagelike structure which appears to be frozen in as the nematic phase solidifies. Also, it would be consistent with longer range orientation-dependent interactions acting on the probe than on the rodlike solvent molecules. This mechanism of a probe or solute molecule reorienting relative to a persistent potential, which then relaxes on a slower time scale, is expected to be a very general one in liquid crystals and plastic crystals, structured liquids, and biological systems.

It would, of course, be of considerable interest to study the effects of the size and the shape of a variety of spin probes on both the molecular ordering as reflected in γ_P', as well as on the molecular dynamics and the proposed SRLS mechanism. Such experiments are currently planned.

Acknowledgments. We wish to acknowledge helpful discussions with Dr. C. F. Polnaszek. We wish to thank Mr. R. E. Terry for his considerable help in constructing the high pressure vessel.

References and Notes

(1) Supported in part by a grant from the National Science Foundation and by the Cornell University Materials Science Center.
(2) (a) S. A. Goldman, G. V. Bruno, C. F. Polnaszek, and J. H. Freed, *J. Chem. Phys.*, **56**, 716 (1972); (b) S. A. Goldman, G. V. Bruno, and J. H. Freed, *ibid.*, **59**, 3071 (1973).
(3) J. S. Hwang, R. P. Mason, L. P. Hwang, and J. H. Freed, *J. Phys. Chem.*, **79**, 489 (1975).
(4) J. H. Freed in "Spin Labelling Theory and Applications", L. J. Berliner, Ed., Academic Press, New York, N.Y., 1975, Chapter 3.
(5) C. F. Polnaszek and J. H. Freed, *J. Phys. Chem.*, **79**, 2283 (1975). Hereafter referred to as I.
(6) D. S. Lenlart, H. D. Connor, and J. H. Freed, *J. Chem. Phys.*, **63**, 165 (1975).
(7) J. Jonas, *Adv. Magn. Reson.*, **6**, 73 (1973).
(8) J. Jonas, *Ann. Rev. Phys. Chem.*, **26**, 167 (1975).
(9) J. S. Hwang, D. Kivelson, and W. Z. Plachy, *J. Chem. Phys.*, **58**, 1753 (1973).
(10) B. Deloche, B. Cabane, and D. Jerome, *Mol. Cryst. Liq. Cryst.*, **15**, 197 (1971).
(11) J. R. McColl, *Phys. Lett.*, **38A**, 55 (1972).
(12) J. R. McColl and C. S. Shih, *Phys. Rev. Lett.*, **29**, 85 (1972).
(13) W. Z. Plachy and T. J. Schaafsma, *Rev. Sci. Instrum.*, **40**, 1590 (1969).
(14) W. T. Doyle, T. F. Dutton, and A. B. Wolbarst, *Rev. Sci. Instrum.*, **43**, 1668 (1972).
(15) P. W. Bridgman, "The Physics of High Pressure", Dover Publications, New York, N.Y., 1970.
(16) The high pressure vessel has held a pressure of 5 kbars for 1 month with no noticeable change.
(17) J. C. Lang, Jr., and J. H. Freed, *J. Chem. Phys.*, **56**, 4103 (1972). Equation A1 of that reference is given incorrectly, but the actual analysis used the correct expressions. The correct form of eq A1 is

$$\left[\left[\Delta\omega_{N,M} - i\left[T_2(0)^{-1} + \omega_{HE}\left(1 - \frac{1}{3}P_M\right)\right]\right]\bar{Z}_{N,M} + i\omega_{HE}\frac{1}{3}P_M\sum_{M'\neq M}\bar{Z}_{N,M'} = D_{M,A}\right.$$

We wish to thank Mr. A. E. Stillman for helpful correspondence on this point.
(18) L. P. Hwang and J. H. Freed, *J. Chem. Phys.*, **63**, 118 (1975).
(19) W. Maier and A. Saupe, *Z. Naturforsch. A*, **13**, 564 (1958); **14**, 882 (1959); **15**, 287 (1960).
(20) P. G. de Gennes, "The Physics of Liquid Crystals", Oxford University Press, New York, N.Y., 1974.
(21) (a) S. Chandrasekhar and N. V. Madhusudana, *Acta Crystallogr., Sect. A*, **27**, 303 (1971); (b) *Mol. Cryst. Liq. Cryst.*, **24**, 179 (1973).
(22) (a) R. L. Humphries, P. G. James, and G. R. Luckhurst, *J. Chem. Soc., Faraday Trans. 2*, **68**, 1031 (1972); (b) R. L. Humphries and G. R. Luckhurst, *Chem. Phys. Lett.*, **17**, 514 (1972).
(23) G. R. Luckhurst and M. Setaka, *Mol. Cryst. Liq. Cryst.*, **19**, 279 (1973). We employ the notation similar to that of these authors.
(24) L. Onsager, *Ann. N.Y. Acad. Sci.*, **51**, 627 (1949).
(25) J. R. McColl, *J. Chem. Phys.*, **62**, 1593 (1974).
(26) D. Eden, C. W. Garland, and R. C. Williamson, *J. Chem. Phys.*, **58**, 1861 (1973).
(27) J. Mayer, T. Waluga, and J. A. Janik, *Phys. Lett.*, **41A**, 102 (1972).
(28) J. A. Janik et al., *J. Phys. (Paris)*, Colloquium CI, 159 (1975).
(29) M. J. Press and A. S. Arrott, *Phys. Rev.*, **8A**, 1459 (1973).
(30) E. Gulari and B. Chu, *J. Chem. Phys.*, **62**, 795 (1975).
(31) The graphs in Figure 5 do not include the results on the pressure sample used for the 7.7 °C runs. The results for $S^{(p)}$ from this sample are systematically 0.005 too low for agreement with the atmospheric pressure samples of I and with the other pressure samples. This could be due to an impurity in this high pressure sample. This small deviation is not of significant importance in the relaxation studies.
(32) Y. S. Lee, Y. Y. Hsu, and D. Dolphin, *Liq. Cryst. Ordered Fluids*, **2**, 357 (1974).
(33) C. F. Polnaszek, Ph.D. Thesis, Cornell University, 1976. Note eq 2.18d of ref 5 has a misprint: $2R_\perp\lambda/7$ should replace $2R_\parallel\lambda/7$. It appears correctly in this reference and in ref 4.
(34) J. G. Powles and M. C. Gough, *Mol. Phys.*, **16**, 349 (1969).
(35) (a) R. L. Armstrong and P. A. Speight, *J. Magn. Reson.*, **2**, 141 (1970). (b) The spectra obtained with the high pressure apparatus are slightly asymmetric. Also there is a small amount of base line shift. We partially compensated for both these effects in our simulations. However, small discrepancies resulting from these effects do show up in our comparisons between the experimental and simulated spectra in Figures 9–11.
(36) In I it was pointed out that one could estimate an ϵ' from this mechanism. It would only apply to $j_0(\omega)$ and not to $j_2(\omega)$. One obtains

$$j_0(\omega) \approx j_0(0)[1 + \epsilon'\omega^2\tau_R^2]^{-1}$$

with

$$\epsilon' \approx 1 + S_I^2(\tau_X^3/\tau_R^3)\frac{1 + \omega^2\tau_R^2}{1 + \omega^2\tau_X^2}$$

which is appropriate for $(\tau_R/\tau_X)^2 \ll 1$ and $S_I^2\tau_X/\tau_R < 1$. This form is a little more accurate than given in I.
(37) Very rapidly relaxing torque components can be expected to induce angular momentum, hence spin rotational, relaxation (given by τ_J) without substantially affecting the overall reorientation. This may be the explanation for the anomalies in the product $\tau_R\tau_J$ observed in ref 6.
(38) (a) P. G. de Gennes, *Mol. Cryst. Liq. Cryst.*, **7**, 325 (1969); (b) P. Pincus, *Solid State Commun.*, **7**, 415 (1969).
(39) J. W. Doane, C. E. Tarr, and M. A. Nickerson, *Phys. Rev. Lett.*, **33**, 620 (1974).
(40) We have attempted to simulate a spectrum obtained at 2000 bars and 7.7 °C with an estimated $\tau_R \sim 7 \times 10^{-9}$ s. The value of ϵ' required seemed to be greater than 1, but less than 13. The intensity ratio of the lines in the experimental spectrum was found to change with time. Hence no reliable value of ϵ' could be obtained.
(41) A closely related observation for DTBN in the plastic crystal camphene has recently been made by Glarum and Marshall, *J. Chem. Phys.*, **62**, 956 (1975).